original paper

Raw Iron Tree Seeds for the Removal of Methyl Orange Dye from Synthetic Aqueous Solution

of methyl orange (MO) dye from aqueous solutions by raw *Prosopis africana* (RPA) was investigated using a batch system under controlled conditions. The point of zero charge (PZC) of raw *Prosopis africana* (RPA) was found to be pH 6. The raw *Prosopis africana* (RPA) was characterized by Fourier transform infrared spectroscopy (FTIR) and scanning electron microscopy (SEM) methods to confirm the adsorption of MO dye onto RPA adsorbent. The kinetic data for the adsorption process evaluated was best described by pseudo-second order in relation to other models studied. Adsorption parameters such as effect of pH, contact time, adsorbent dosage and initial concentration were studied for optimization purposes. The adsorption isotherm for the processes was also estimated and established. The adsorption data fitted well the Freundlich isotherm model relative to other models tested. Thermodynamic studies revealed that the adsorption processes were exothermic and feasible in nature. This indicates that raw *Prosopis africana* (RPA) can be a promising adsorbent for the removal of hazardous dye from synthetic wastewater.

Keywords: Adsorption, kinetic, thermodynamic, Isotherms, Prosopis africana.

INTRODUCTION

Disposal of aqueous chemical waste as effluent into wastewater by many manufacturing industries is a challenge to most developing nations (Ali et al. 2012; Yu et al. 2014). Some of the organic contaminants released into water bodies are acutely toxic and hazardous in nature (Ali et al. 2012). The most common organic contaminants responsible for environmental pollution are dyes, pesticides, pharmaceuticals/drugs, phenols and aromatic amines (Yu et al. 2014). Several

methods have been reported in literature for treating such contaminants, which include the use of adsorbents. Most common adsorbents used for the removal of pollutants are carbon, zeolites, polymers, biomass, siliceous materials, agricultural wastes and industrial by-products (Krysztafkiewicz et al. 2002). Adsorption by carbon has been proved to be an efficient method for the removal of a variety of organic and inorganic contaminants of concern from waste water systems which include naphthenic acids (NA), ammonia, chromium (VI), sulfates, aromatic hydrocarbons, and trace metals. The properties of activated carbon such as the high surface area, well-developed pore structure and the presence of functional group on their surface make them promising adsorbents (Hansen and Davies, 1994). Superior removal percentage of soluble and insoluble pollutants even at lower concentrations, availability and cost effectiveness, flexibility and safety in design and operation, sensitivity to the presence of toxic contaminants, ability to regenerate and reuse the adsorbents and ability to be used in batch or continuous mode are the advantages of using carbon based adsorbents for adsorption purposes (Ali et al. 2012).

Iron tree *(Prosopis Africana),* family Mimosaceae, is a perennial leguminous woody tree of about 70 feet high mostly found growing in the savanna regions of West Africa (Kolapo et al. 2009). It has very hard stem that is used in different parts of Nigeria for making boats, pestle and wooden gong; its fermented seeds are used as food condiment/flavouring agent (Aremu et al. 2006). Its young leaves and shoots are folders highly sought after towards the end of the dry season and the gum from the seed mesocarp possesses drug delivery properties (Agboola, 2004).

This work is aimed at investigating the potentials of raw Iron tree seeds for the removal of methyl orange dye (Figure 1) from synthetic aqueous solution through batch adsorption processes. This is intended to be achieved through the study of adsorption, kinetic and

thermodynamic properties of the interaction between the methyl orange (MO) dye molecules and the raw iron tree (RPA) adsorbent.

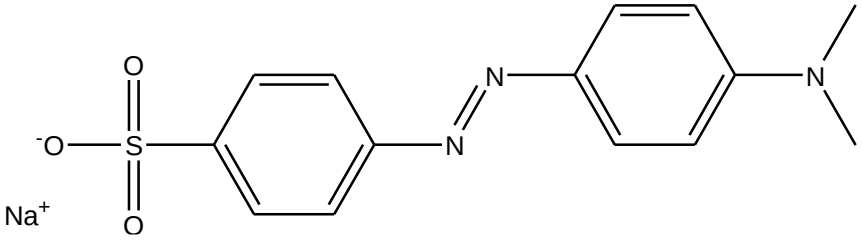

Figure 1. Structure of Methyl orange (sodium 4-[(4-dimethylamino)phenylazo]benzenesulfonate)

MATERIALS AND METHODS

Plant Material Collection and Adsorbent Preparation

Sample of Iron tree seed were collected from farmland in Akpuuna 1, Mbaterem, Ukum Local Government area of Benue State, Nigeria. Samples were packaged in clean polythene bags and transported to the laboratory. The removed seeds from the pods were thoroughly washed with water to remove dust and other impurities. These seeds were then air-dried to the constant mass in the laboratory as described by Oyeyode and Ayuba (2022). The dried seeds were then pulverized and sieved into fine particles as previously described by Akintola et al. (2015). The final product (Figure 2) was stored in a clean, air-tight container for further usage as adsorbent for subsequent characterization analysis and batch adsorption experiments.

Figure 2. Fine particles of Iron tree as adsorbent

Preparation of Methyl Orange Dye Solution

The stock solution of Methyl orange dye was prepared by dissolving accurately 1g of the dye into a 1L to produce 1000 mgL^{-1} using distilled water. The experimental solutions of desired concentration were prepared accordingly by diluting the stock solution with distilled water. The concentration of the un-adsorbed MO dye was measured at λmax = 463.39 nm using UV–visible spectrophotometer (Model Hitachi 2800).

Characterization of the Adsorbent Surface

The surface morphological properties of the adsorbent (RPA) sample were investigated using Scanning Electron Microscope (Phenom World Eindhoven). Scanned micrographs of adsorbent before and after adsorption of MO dye were taken at an accelerating voltage of 15.00 kV and x500 magnification. Fourier Transform Infrared (FTIR) analysis of the RPA adsorbent before and after adsorption of MO dye were carried out using Cary 630 Fourier Transform Infrared Spectrophotometer Agilent Technology. The analysis was done by scanning the sample through a wave number range of 650 – 4000 cm^{-1}; 32 scans at 8cm^{-1}resolution.

Salt addition method was applied to determine the RPA point of zero charge (PZC) as reported by Tahira et al. (2011). PZC values for RPA was determined in 0.1 M $NaNO_3$ solution at 303-333K. 0.2 g of RPA sample was added to 40.0 mL of 0.1 M $NaNO_3$ solution. The pH of the suspension was then adjusted with 0.1 M HCl and 0.1 M NaOH 0.1 using pH-meter (MP 220) to obtain an initial pH value of 2, 4, 6, 7, 8 and 10. Each flask was then vigorously agitated in a shaker bath for 24 h. After settling, the final pH of each suspension was measured very carefully. The ΔpH (the difference between final and initial pH) values were then plotted against the initial pH values. The initial pH at which ΔpH is zero was taken to be the PZC.

Batch Adsorption Experiments

Batch experiments were carried out to determine the optimum conditions for the equilibrium adsorption of Methyl orange onto RPA. Experimental parameters including contact time, adsorbent dosage, initial dye concentration and initial solution pH were optimized. The results obtained after the optimization experiments were used to conduct the batch adsorption experiments. Each of these systems were separately run in a 120 cm^3 plastic bottle differently at 30^O, 40^O, 50^O and 60^OC respectively. The plastic bottles were tightly covered during the equilibration period and placed on a temperature controlled water bath shaker (SHA-C Model) for the optimized period. After reaching adsorption equilibrium, the content was filtered through Whatman No 1 filter paper. The filtrate was analyzed using Perkin-Elemer Uv-visible spectrophotometer at maximum absorbance wavelength of 463.39 nm (Adekola et al. 2011; Vibhawari and Pandey, 2012). The adsorption capacity was calculated using equation (1)

$$q_e = \frac{(C_o - C_e)V}{m} \qquad (1)$$

Where; C_o and C_e are the initial and equilibrium concentration (mgl^{-1}) respectively of Methyl orange in solution, V is the volume of Methyl orange solution (L), and m is the mass (g) of the adsorbent.

RESULTS AND DISCUSSION

Surface Characterization of the Adsorbent

FTIR analysis of adsorbents before (RPA) and after adsorption (RPA-MO) was carried out using Cary 630 Fourier Transform Infrared Spectrophotometer Agilent Technology. The analysis was done by scanning the sample through a wave number range of 650 – 4000 cm^{-1}; 32 scans at $8cm^{-1}$ resolution and the reported in Figure 3. The FTIR spectra analysis results as presented in Table 1 indicate that only minor differences between before and after adsorption of MO dye on RPA adsorbent could be established. However, shift in absorption bands and changes in wavelength between the before and after adsorption of MO dye indicate that Methyl orange have been adhered on the surface of the RPA.

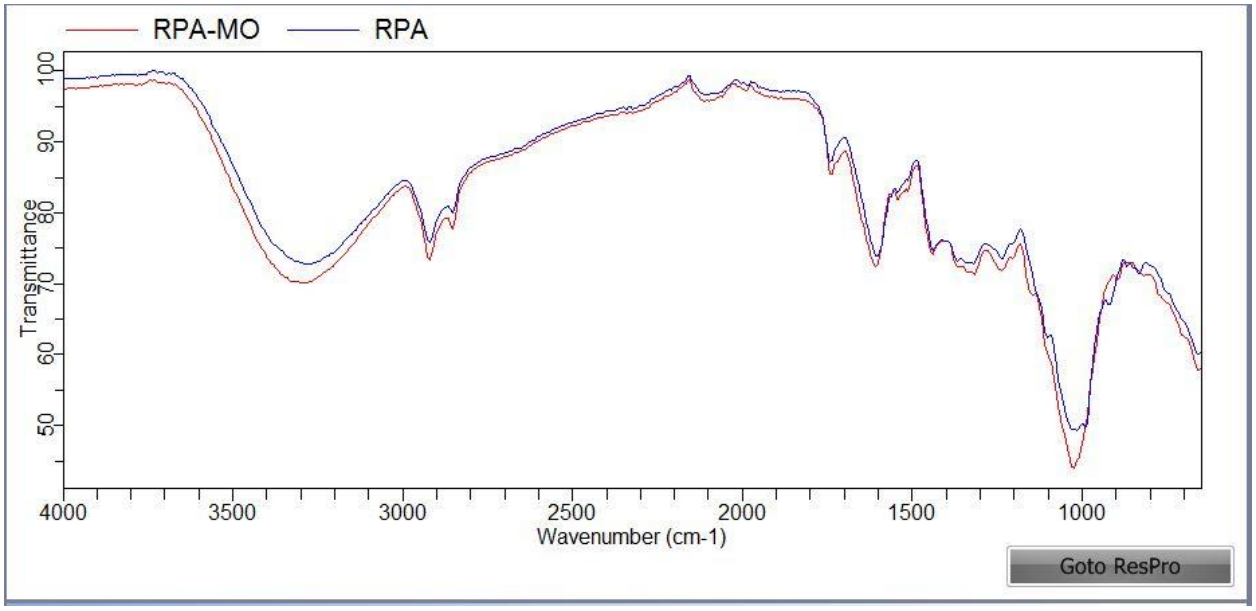

Figure 3. FTIR spectral of RPA before and after adsorption of MO

Table 1. Functional groups recognized before and after adsorption of MO dye onto RPA

Functional Group	Absorption range (cm^{-1})	Absorption intensity	Before adsorption (cm^{-1})	After adsorption onto MO(cm^{-1})	Difference (cm^{-1})
Alcohol (-OH)	3400-3700	Strong, broad	3272	3301	+29
Alkane (C-H)	2850-2975	Medium to strong	2921	2925	+4
Ester (RCOOR)	1735-1750	Strong	1745	1741	-4
Alkyne (C≡C)	2100-2250	Medium	2113	2113	0
Alcohol (R-OH)	1000-1305	Medium	1019	1030	+11
Aromatics	1650-2000	Weak	1990	-	-

Scanning Electron Microscopy (SEM) of the RPA adsorbent before and after adsorption were taken at an accelerating voltage of 15.00kV and x500 magnification. Scanned micrograph images of the adsorbent before and after adsorption of the dye is presented in Figure 5. It be observed from the surface morphology of RPA before adsorption to contain some cavities and pores which may enhance adsorption and intra-particle diffusivity. The micrograph of RPA after adsorption of MO shows depositions of adsorbed dyes in smooth regular formations on the surfaces. The porous structures on the surface of the adsorbent however have been filled after adsorption of the MO dye. Similar findings were reported by Idoko and Ayuba (2020) for the adsorption of Crystal violet dye from aqueous solution using activated Cowpea (*Vigna Unguiculata)* husk as adsorbent.

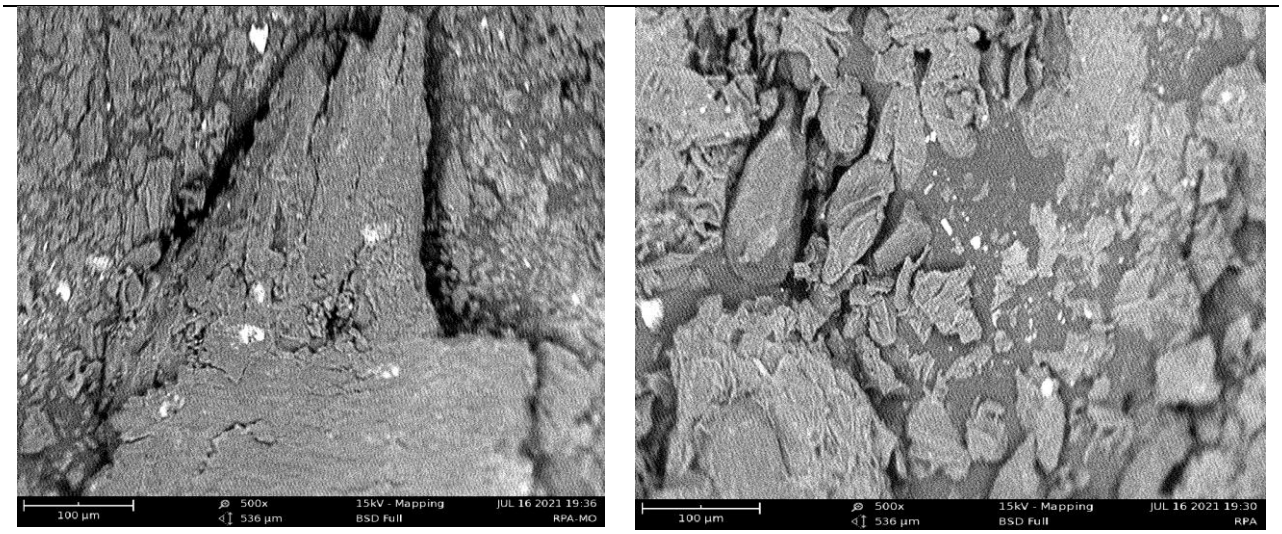

(a) **(b)**

Figure 4. SEM Micrograph of RPA (a) before and (b) after adsorption of MO

The results of the point of zero charge of the RPA adsorbent is as presented in Figure 5. From the figure, the PZC of RPA was found to be pH 6.00. The significance of these plots for adsorbents surfaces will have positive charge at solution pH values less than the PZC and thus be a surface on which anions may adsorb. On the other hand, that surface will have negative charge at solution pH values greater than the PZC and thus be a surface on which cations may adsorb.

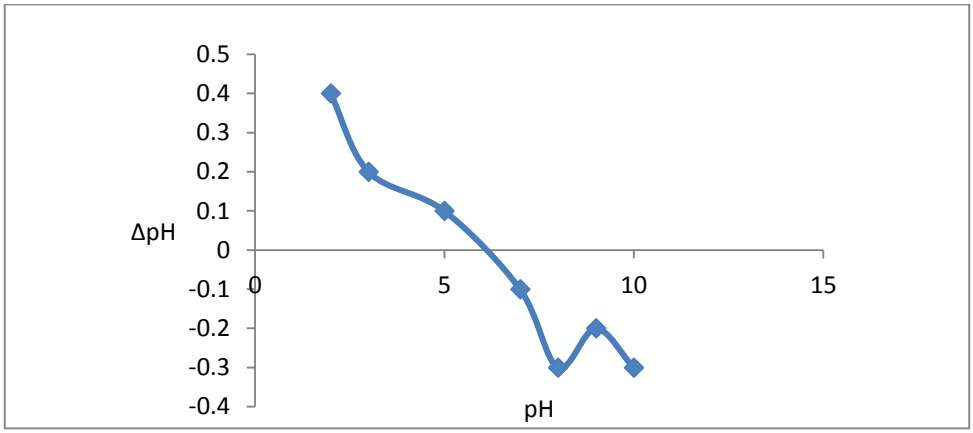

Figure 5. Point of zero charge (PZC) of RPA adsorbent

Batch Adsorption

Fig. 6a shows plots of the effect of contact time on adsorption of MO dye onto RPA adsorbent. MO dye show rapid onto RPA adsorption within 60 minutes of contact time due to the easy accessibility of the adsorption sites on the adsorbent and was followed by decreased of MO dye adsorption at longer contact time. The rate of adsorption indicated that the quantity adsorbed of 2.46 $mg.g^{-1}$ was observed in the first 60 min of contact time. The initial rapid phase may also be due to the increased number of vacant sites available at the initial stage where as after 60 min decreasing effect is due to vacant surface sites not easily occupied due to repulsive forces. At a later time, the process becomes relatively slower and equilibrium conditions are believed to be reached at 60 min. At this point, the amount of MO dye desorbing from the adsorbent is in a stage of dynamic equilibrium with the amount of the dyes being adsorbed onto the adsorbents. The time required to attain this state of equilibrium is termed the equilibrium time, and the amount of MO dye adsorbed at the equilibrium time reflects the maximum adsorption capacity of the adsorbent under those operating conditions (Satish et al. 2011). Similar trend was observed by Mitiku (2015) for the removal of 2,4-D-atrazine and major metabolites of atrazine from aqueous solution by Fe-Zr-Mn nano composite.

The adsorbent dosage is an important parameter because it determines the capacity of the adsorbent for a given initial dye concentration. Figure 6b showed that as the adsorbent dosage increased, the amount adsorbed also increased but the amount adsorbed per unit mass of the adsorbent decreased considerably for MO dye. The decrease in adsorption per unit mass with increasing dosage of adsorbent is attributed to possible overlapping of adsorption sites as adsorbent dosage increases, the adsorbent which will equally reduce the effective adsorption sites. The amount of MO dye molecules adsorbed is dependent upon the initial concentration,

and at higher concentrations, the available sites of adsorption become fewer (Mitiku, 2015). From Figure 6b, it was observed that as the adsorbents dose increased from 0.02 to 0.3g, the quantity adsorbed ($mg.g^{-1}$) decreased from 25.68 to 1.59. This showed the high adsorption capacity of MO dye at low dosage. The removal of lead (II) and copper (II) ions from aqueous solution by Baobab (*Adononsia digitata*) fruit shells biomass followed similar trend as reported by Chigongo et al. (2013). Also, in another study, Coconut coir dust as a low cost adsorbent for the removal of cationic dye from aqueous solution showed similar trends (Etim et al. 2016)

One of the most important and widely studied aspects of adsorption of organic pollutants in aqueous solution is the effect of solute concentration on adsorption affinity, given that, in theory, this should convey important information about adsorption mechanisms. As given in Figure 7c, it was observed that as the initial concentration was increased, the amount of MO dye adsorbed on RPA also increased. At low concentration, the available driving force for transfer of MO molecules onto the adsorbent particles is low, while at high concentration, there is a corresponding increase in the driving force, thereby enhancing the interaction between the MO dye molecules in the aqueous phase and the active sites of the adsorbents. As a result of this, there was an increase in the uptake of MO dye molecules. Similar trends were reported on Coconut coir dust as a low cost adsorbent for the removal of cationic dye from aqueous solution by Etim et al. (2016).

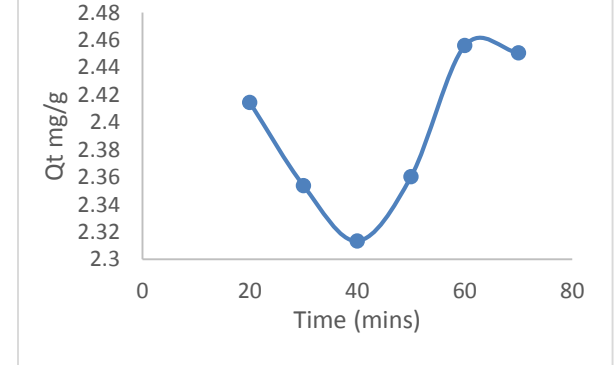

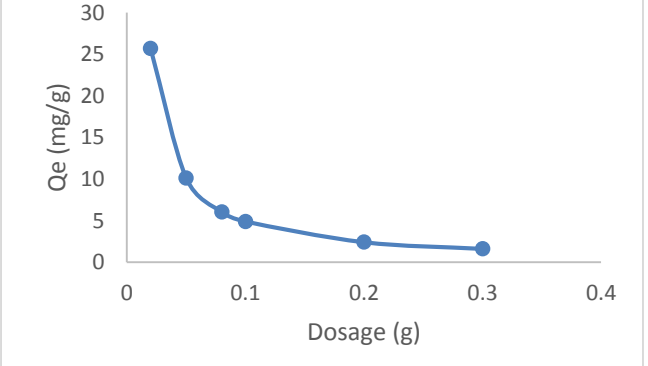

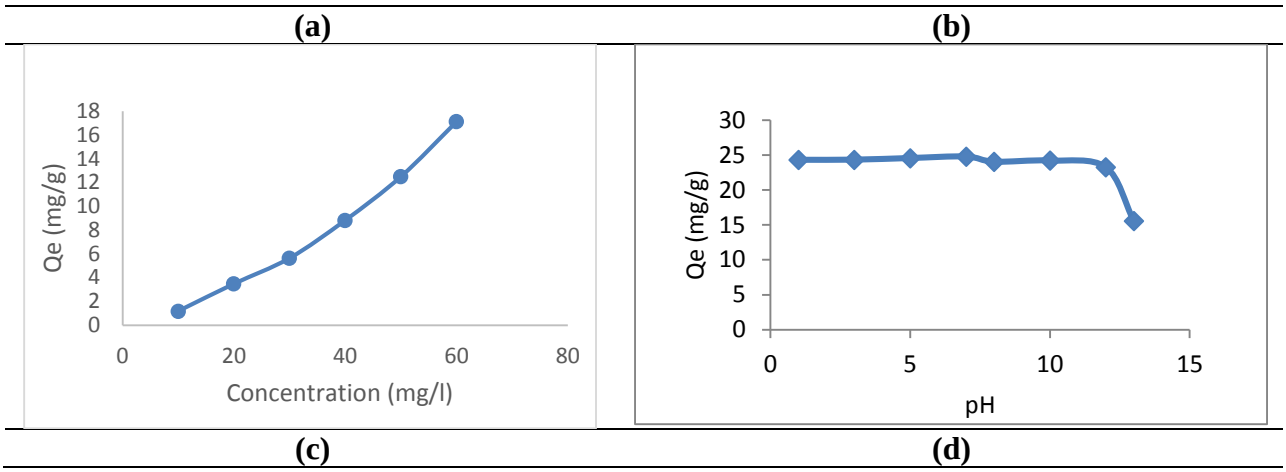

Figure 6. Effect of (a) contact time, (b) adsorbent dosage, (c) initial dye concentration, (d) pH on the adsorption of MO onto the RPA

Figure 6d shows plots of variation of the amount of MO dye adsorbed onto RPA with pH. The effect of pH of solution on MO dye removal were evaluated by varying the pH of solution from 1 to 13. It was observed that the maximum adsorption of MO dye onto RPA occurred at pH 7. It can be observed from the plot that RPA showed good removal in neutral medium condition. The decrease in the adsorption capacity of MO dye as pH values increase (7.0 - 13.0) could be related to the repulsion between the negative charge of anionic species in solution and negative surface charge of the adsorbent (Esmaeili and Beni, 2005; Kumar et al. 2006). Similar work was reported on biosorption of toxic heavy metals from aqueous solution by *Ulva lactuca* activated carbon reported by Wael et al. (2016) and that of the adsorption of zinc (II) on magnetite onto Baobab (*Adansonia digitata*) and magnetite-baobab composite adsorbents (Abdus-Salam and Adekola, 2018).

Adsorption Kinetics

(a) The pseudo first-order equation

The pseudo first-order equation (Lagergren, 1898) is generally expressed as follows:

$$\frac{\partial q_t}{\partial_t} = k_1(q_e - q_t) \qquad (2)$$

Where q_e and q_t are the adsorption capacity at equilibrium and at time t, respectively ($mg.g^{-1}$), k_1 is the rate constant of pseudo first-order adsorption ($l.min^{-1}$). After integration and applying boundary conditions t = 0 to t = t and $q_t = 0$ to $q_t = q_t$, the integrated form of Eq. (2) becomes:

$$\log(q_e - q_t) = \log(q_e) - \frac{k_1}{2.303} t \qquad (3)$$

The values of $\log(q_e - q_t)$ were linearly plotted against t which should give a linear relationship from which k_1 and q_e can be determined from the slope and intercept of the plot respectively (Figure 7a).

(b) The pseudo second-order equation

The pseudo second-order adsorption kinetic rate equation is expressed as (Lagergren, 1898):

$$\frac{\partial q_t}{\partial t} = k_2(q_e - q_t)^2 \qquad (4)$$

Where k_2 is the rate constant of pseudo second-order adsorption ($g.mg^{-1}min^{-1}$). For the boundary conditions t = 0 to t = t and $q_t = 0$ to $q_t = q_t$, the integrated form of Eq. (4) becomes:

$$\frac{1}{(q_e - q_t)} = \frac{1}{q_e} + k_t \qquad (5)$$

This is the integrated rate law for a pseudo second-order reaction equation (5) can be rearranged to obtain Eq. (6), which has a linear form:

$$\frac{t}{q_t} = \frac{1}{k_2 q_e^2} + \frac{1}{q_e}(t) \qquad (6)$$

If the initial adsorption rate, h ($mg.g^{-1}min^{-1}$) is;

$$h = k_2 q_e^2 \qquad (7)$$

Then equation (6) becomes

$$\left(\frac{t}{q_t}\right) = \frac{1}{h} + \frac{1}{q_e}(t) \qquad (8)$$

The plot of (t/q_t) against t of Equation (8) should give a linear relationship from which q_e and k_2 can be determined from the slope and intercept of the plot respectively (Figure 7b).

(c) Elovich Equation

The Elovich kinetic model is described by the following relation (Guo et al. 2010).

$$q_t = {}^{1}/_{\beta} \ln(\alpha\beta) + \left({}^{1}/_{\beta}\right) lnt \qquad (9)$$

This model gives useful information on the extent of both surface activity and activation energy for chemisorptions process. The parameters (α) and (β) can be calculated from the slope and intercept of the linear plot of q_t versus ln(t) (Figure 7c).

(d) Intraparticle Diffusion Equation

The slower step in an adsorption process is usually taken as the rate determining step. This step is often attributed to pore and intra particle diffusion. Since pseudo first and pseudo second order models cannot provide information on effect of intra particle diffusion in adsorption, intra particle diffusion model can be used (Ahmed and Dhedan, 2012). Possibility of involvement of intra particle diffusion model as the sole mechanism was investigated according to Weber-Morris Equation (10) (Weber and Morris, 1963):

$$q_t = C + K_{int} t^{1_2} \qquad (10)$$

Where the constant K_{int} ($mg.g^{-1}min^{-1/2}$) is the intra particle diffusion rate and C is the boundary layer thickness. If the rate limiting step is only due to the intra particle diffusion, then q_t versus $t^{1/2}$ will be linear and the slope passes through the origin (Figure 7d).

Table 2. Kinetic model parameters for the adsorption of MO onto RPA

Kinetic Models	**Parameters**			
Pseudo-first order	**qe_{Cal}(mg/g)**	**qe_{Exp}(mg/g)**	**K_1(min^{-1})**	**R^2**
	12.353	0.306	0.00	0.003
Pseudo-second order	**qe_{Cal}(mg/g)**	**qe_{Exp}(mg/g)**	**K_1(min^{-1})**	**R^2**

	12.353	12.048	1.722	0.999
Elovich		**B**	**A**	**R^2**
		23.256	8.9×10^{121}	0.037
Intra particle diffusion		**K_3**	C	**R^2**
		-0.012	12.140	0.017

Table 2 shows the parameters obtained from the tested kinetic models for the adsorption of MO dye onto the adsorbent. The pseudo-second-order kinetic model fits the experimental data quite well with a correlation coefficient (R^2) value of almost unity, and the experimental and theoretical adsorption capacities are quite in good agreement. This indicates the applicability of the second-order kinetic model to describe the adsorption process of MO onto the RPA adsorbent.

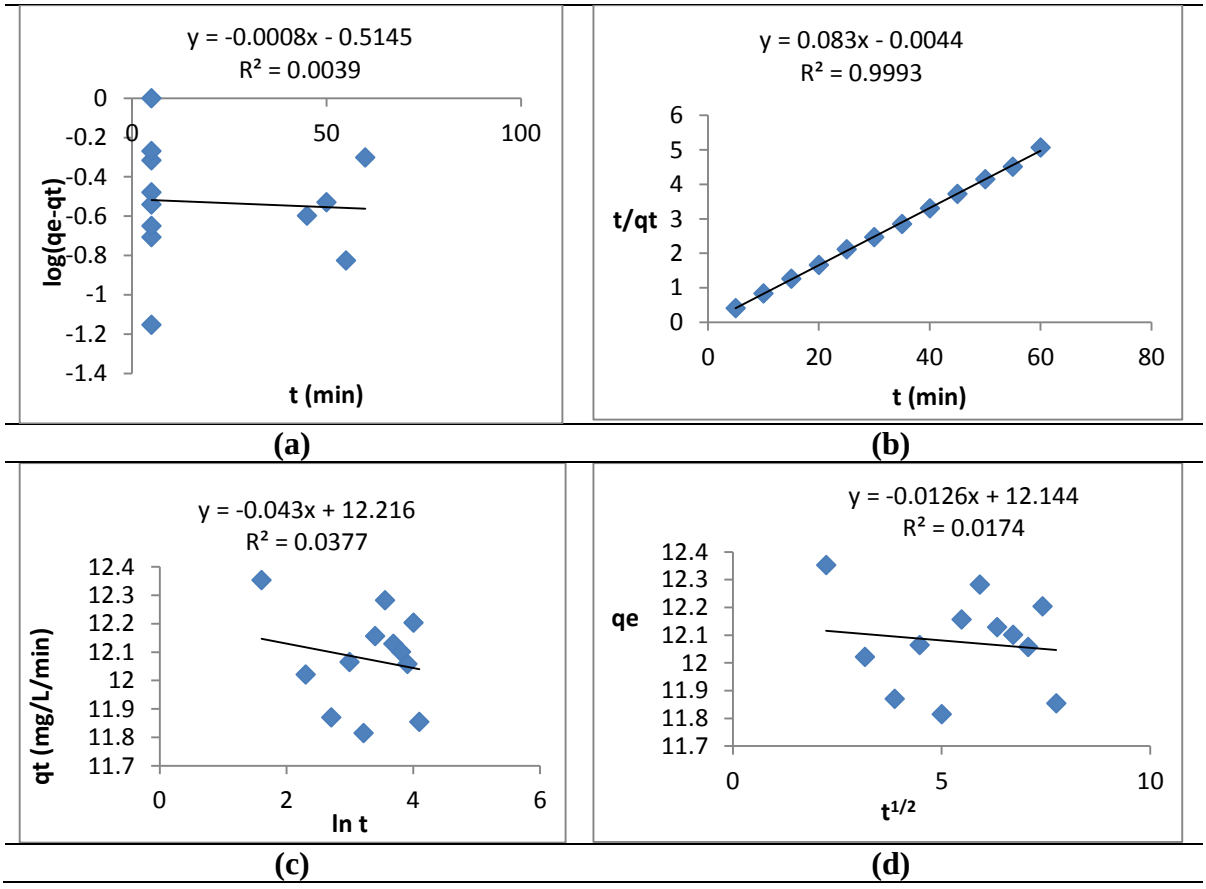

Figure 7. (a) Pseudo-first order (b) Pseudo-second order (c) Elovich (d) Intra particle diffusion plot for adsorption of MO onto RPA

Adsorption Isotherms

The equilibrium adsorption data obtained after adsorption of Methyl orange (MO) dye onto adsorbent (RPA) was fitted into some selected isotherm models to assess which relatively best describe the adsorption process. Isotherms correlate the equilibrium adsorption data with different mathematical models to describe how adsorbates interact with adsorbents and this is critical in optimizing the use of adsorbent (Lagergren, 1898). Four isotherms were tested and the evaluated adsorption isotherm parameters reported in Table 3.

(a) Langmuir Isotherm

This describes quantitatively the formation of a monolayer adsorbate on the outer surface of the adsorbent, and after that no further adsorption takes place. Thereby, the Langmuir represents the equilibrium distribution of dye molecules between the solid and liquid phases (Lagergren, 1898). Langmuir represented the following equations:

$$q_e = \frac{Q_O K_l C_e}{1 + K_l C_e} \qquad (11)$$

Langmuir adsorption parameters were determined by transforming the Langmuir equation (11) into linear form.

$$\frac{1}{\mathrm{q_e}} = \frac{1}{\mathrm{Q_o}} + \frac{1}{\mathrm{Q_o K_l C_e}} \qquad (12)$$

Where C_e is the equilibrium concentration of adsorbate ($mg.l^{-1}$), q_e is the amount of dye adsorbed per gram of the adsorbent at equilibrium ($mg.g^{-1}$), Q_o the maximum monolayer coverage capacity (mg.g-1) and K_l the Langmuir isotherm constant ($L.mg^{-1}$).

The values of q_{max} and K_l were computed from the slope and intercept of the Langmuir plot of $\frac{1}{qe}$ versus $\frac{1}{Ce}$. The essential features of the Langmuir isotherm may be expressed in terms of equilibrium parameter R_L, which is a dimensionless constant referred to as separation factor or equilibrium parameter (Webber and Moris, 1963).

$$R_L = \frac{1}{(1 + K_l C_o)} \qquad (13)$$

Where C_o is the initial concentration, K_l the constant related to the energy of adsorption (Langmuir constant). R_L value indicates the adsorption nature to be either unfavorable if $R_L>1$, linear if $R_L=1$, favorable if $0<R_L<1$ and irreversible if $R_L= 0$.

(b) Freundlich Adsorption Isotherm

This is commonly used to describe the adsorption characteristics for a heterogeneous adsorbent surface (Cabuk et al. 2005). These data often fit the empirical equation proposed by Freundlich:

$$Q_e = K_f C_e^{1/n} \qquad (14)$$

Where K_f is the Freundlich isotherm constant ($mg.g^{-1}$), n is the adsorption intensity, C_e is the equilibrium concentration of adsorbate ($mg.L^{-1}$) and Q_e the amount of metal adsorbed per gram of the adsorbent at equilibrium ($mg.g^{-1}$). Linearizing equation (14), we have:

$$logQ_e = logK_f + \frac{1}{n} logC_e \qquad (15)$$

The constant K_f is an approximate indicator of adsorption capacity, while 1/n is a function of the strength of adsorption in the adsorption process (Faria and Orfao, 2004). If n = 1 then the partition between the two phases are independent of the concentration. If value of 1/n is below one, it indicates a normal adsorption. On the other hand, 1/n being above one indicates cooperative adsorption (Mohan and Karthikeyan, 1997). The function has an asymptotic maximum as pressure increases without bound. As the temperature increases, the constants k and

n change to reflect the empirical observation that the quantity adsorbed rises more slowly and higher pressures are required to saturate the surface. However, K_f and n are parameters characteristic of the adsorbent-adsorbate system, which must be determined by data fitting and whereas linear regression is generally used to determine the parameters of kinetic and isotherm models (Fatt-kassinos et al. 2011). Specifically, the linear least-squares method and the linearly transformed equations have been widely applied to correlate sorption data where 1/n is a heterogeneity parameter, the smaller 1/n, the greater the expected heterogeneity. This expression reduces to a linear adsorption isotherm when 1/n = 1. If n lies between one and ten, this indicates a favorable sorption process (Wahab et al. 2012).

(c) The Temkin Isotherm

This isotherm contains a factor that explicitly takes into account the adsorbent-adsorbate interactions. By ignoring the extremely low and large value of concentrations, the model assumes that heat of adsorption (function of temperature) of all molecules in the layer would decrease linearly rather than logarithmic with coverage (Wahab et al. 2012). As implied in equations 16 and 17, its derivation is characterized by a uniform distribution of binding energies (up to some maximum binding energy). The test of this isotherm was carried out by plotting the quantity adsorbed q_e against $\ln C_e$ and the constants were determined from the slope and intercept. The model is given by the following equation (Lagergren, 1898).

$$q_e = \frac{RT}{b_T}\ln(A_T C_e) \qquad (16)$$

$$q_e = \frac{RT}{b_T} lnA_T + \left(\frac{RT}{b_T}\right) lnC_e = BlnA_T + \left(\frac{RT}{b_T}\right) lnC_e \qquad (17)$$

$$B = \frac{RT}{b_T} \qquad (18)$$

Where A_T is the Temkin isotherm equilibrium binding constant ($L.g^{-1}$), b_T is the Temkin isotherm constant, R is the universal gas constant (8,314 $J.mol^{-1}K^{-1}$), T the temperature at 298K and B is the constant related to heat of adsorption ($J.mol^{-1}$).

(d) Doubinin-Radushkevich Isotherm

Dubinin-Radushkevich isotherm is generally applied to express the adsorption mechanism with a Gaussian energy distribution onto a heterogeneous surface (Dabrowski, 2001; Gunay et al. 2007). The model has often successfully fitted high solute activities and the intermediate range of concentrations data well.

$$q_e = (q_s)\exp(-K_{ad}\varepsilon^2) \qquad 19)$$

$$lnq_e = \ln(q_s) - (K_{ad}\varepsilon^2) \qquad (20)$$

Where q_e is the amount of adsorbate in the adsorbent at equilibrium ($mg.g^{-1}$), q_s is the theoretical isotherm saturation capacity ($mg.g^{-1}$), K_{ad} is the Dubinin-Radushkevich isotherm constant ($mol^2.KJ^{-2}$) and ε is the Dubinin-Radushkevich isotherm constant.

The approach is usually applied to distinguish the physical and chemical adsorption of dyes molecules with its mean free energy, E per molecule of adsorbate (for removing a molecule from its location in the adsorption space to the infinity) can be computed by the relationship inequation (21) (Dubinin, 1960; Hobson, 1969).

$$E = b\left[\frac{1}{\sqrt{2B_{DR}}}\right] \qquad (21)$$

Where B_{DR} is denoted as the isotherm constant. Meanwhile, the parameter ε can be calculated using (22):

$$\varepsilon = RTln\left[1 + \frac{1}{C_e}\right] \qquad (22)$$

Where R, T and C_e represent the gas constant (8.314 $J.mol^{-1}K^{-1}$), absolute temperature (K) and adsorbate equilibrium concentration ($mg.L^{-1}$), respectively. One of the unique features of the Dubinin-Radushkevich (DRK) isotherm model lies on the fact that it is temperature-dependent, which when adsorption data at different temperatures are plotted as a function of logarithm of amount adsorbed versus the square of potential energy. All suitable data will lie on the same curve, named as the characteristic curve (Cabuk et al. 2005). From Table 3, when the correlation coefficient (R^2) values were compared, Freundlich adsorption isotherm was found to best fit the adsorption data with an R^2 value of 0.993. The E value obtained from the DKR adsorption isotherm further revealed that the adsorption process is physical with values less than 8kJ/mol.

Table 3. Calculated isotherm constants for the adsorption of MO dye onto RPA

Parameter	**Values**
Langmuir	
Q_O(mg/g)	3.704
K_L(L/mg)	0.033
R_L	0.338
R^2	0.983
Freundlich	
1/n	0.493
n	2.027
k_f	0.018
R^2	0.993
Temkin	
A_T	0.122
b_T	231.124
B	10.900

R^2	0.752
Dubinin-Radushkevich	
q_m(mg/g)	13.158
K_{dr}(mol^2/kJ^2)	3.0×10^{-5}
E(kJ/mol)	0.129
R^2	0.862

Adsorption Thermodynamic Studies

Effect of temperature on Methyl orange dye adsorption onto RPA adsorbent was evaluated by varying the temperature from 303-333K and by keeping all parameters (pH, adsorbent dosage, contact time and initial Methyl orange concentrations) at optimized values. The thermodynamic parameters of adsorption such as changes in free energy (ΔG), enthalpy (ΔH) and entropy (ΔS), and also activation energy which was obtained from Arrhenius equation, give useful view about the feasibility and the spontaneous nature of the adsorption process and generally can be obtained from the following equations:

$$\Delta G = -RTLnK_c \quad (23)$$

$$lnK_c = \frac{\Delta S}{R} - \frac{\Delta H}{RT} \quad (24)$$

$$lnK_c = lnA - \frac{E_a}{RT} \quad (25)$$

Where R is the gas constant (8.314 J.mol^{-1}K^{-1}), T is the absolute temperature (K), E_a is the activation energy, A is the pre-exponential factor and K_c is the thermodynamic equilibrium constant and can be obtained from the relation in equation (26) (Oyeyode and Ayuba, 2022):

$$K_c = \frac{C_a}{C_e} \quad (26)$$

Where C_a is mg of MO dye adsorbed per liter and C_e is the equilibrium MO dye concentration of solution ($mg.L^{-1}$). Both ΔH and ΔS can be obtained from the slope and intercept of Van't Hoff plot using equation (24) of $\ln K_c$ versus 1/T. The activation energy of adsorption, E_a was obtained from the slope of equation (25) by plotting $\ln K_c$ against 1/T.

The negative values of ΔH (Table 4) indicate that the adsorption process is exothermic and adsorption will be favourable at low temperatures. The negative values of ΔH are better described with physisorption (< $41.80 kJmol^{-1}$) the process decrease with increase in temperature. (Aroguz, 2006). The corresponding value of ΔS is negative for adsorption of MO dye onto RPA indicating a decrease in degree of randomness. The ΔG values are all negative at the range of studied temperatures for the adsorption of MO dye onto RPA. The decreasing values imply increasing driving force of adsorption, spontaneity and thermodynamically favorable adsorption (Aroguz, 2006). The lower ΔG values may justify the higher efficiency of RPA towards the removal of MO dyes from aqueous solution.

Table 4. Thermodynamic parameters for the adsorption of Methyl orange (MO) dye onto RPA

T (K)	**K_c**	**ΔG(kJ/mol)**	**ΔH (kJ/mol)**	**ΔS (J/mol.K)**
303	0.939	-0.159		
313	0.930	-0.190	-0.650	-2.677
323	0.918	-0.230		
333	0.919	-0.234		

CONCLUSION

The search for an alternative low-cost and environmentally friendly adsorbent, suitable for the removal of toxic dyes from contaminated wastewater provided the impetus for this research work. Performance characteristics of Methyl orange dye removal from aqueous solution by adsorption onto raw *Prosopis africana* seed were evaluated by investigating the kinetics,

equilibrium, isotherms and thermodynamic of the adsorption system. It was observed that the adsorption process involves a feasible, spontaneous, second order kinetics reflecting a multilayer and physical adsorption process.

ACKNOWLEDGEMENT

The authors wish to thank all the technical staff of Chemistry Laboratory, (Bayero University Kano) for their willingness and readiness to assist at all times in the research laboratory during the conduct of this work.

REFERENCES

Abdus-Salam N, Adekola, SK. (2018). Adsorption studies of zinc (II) on magnetite, baobab (*Adansonia digitata*) and magnetite-baobab composite. Applied Water Science, 218-222.

Adekola FA, Abdus-Salam N, Abdul-Rauf LB. (2011). Removal of arsenic from aqueous solution by synthetic hematite. Journal of Chemical Society Nigeria, 36(2): 52-58.

Agboola DA (2004). *Prosopis africana* (mimosaceae): Stem, roots and seeds in the economy of the savanna areas of Nigeria. Econom. Bot. 58: S34-S42.

Ahmed M J, Dhedan, SK. (2012). Equilibrium isotherms and kinetics modelling of methylene blue adsorption on agricultural wastes-based activated carbons. Fluid phase Equilibria: 317: 9-14. doi: 10. 10`16/j. fluid. 2011. 12.026.

Akintola JK, Ibrahim A, Chadi AS. (2015). Kinetic and Equilibrium studies of Congo Red Adsorption on Adsorbent from Bambara Groundnut Hulls. Al-Hikmah Journal of Pure & Applied Sciences, 2(2), 79-88.

Ali I, Asim M, Khan TA. (2012). Low cost adsorbents for the removal of organic pollutants from Wastewater. Journal of environmental management, 113: 170-183.

Aremu MO, Olonisakin A, Atolaye BO, Ogbu CF. (2006). Some nutritional and functional studies of *Prosopis africana*. Electron. J. Environ. Agric. Food Chem. 5:1640-1648.

Aroguz Z. (2006). Kinetics and thermodynamics of adsorption of azinphosmethyl from aqueous solution onto pyrolyzed (at 600 degrees C) ocean peat moss (Sphagnum sp.). Journal of Hazardous Materials, 135(1-3):100-5. doi:10.1016/j.jhazmat.2005.11.027.

Cabuk A, Ilhan SC, Caliskan F. (2005). Pb^{2+}biosorption of pretreated fungi biomas. Turkish journal of biology. 29(1): 23-28.

Chigongo F, Nyamunda BC, Sithole SC, Gwatidzo L. (2013). Removal of lead (II) and copper (II) ions from aqueous solution by baobab (*Adononsia digitata*) fruit shells biomass. IOSR J Appl Chem: IOSR-JAC 5(1): 43-50.

Dabrowski A. (2001). Adsorption –from theory to practice, Adv. Colloid Interface Sci. 93: 135-234.

Dubinin MM. (1960). The potential theory of adsorption of gases and vapour for adsorbents with energetically non-uniform surface. Chem. Rev, 60: 235-266.

Esmaeili A, Beni AA. (2005). Biosorption of nickel and cobalt from plant effluent by Sargassum glaucescens nanoparticles at new membrane reactor. International Journal of Environmental Science Technology, 12: 2055-64.

Etim UJ, Umoren SA, Eduok UM. (2016). Coconut coir dust as a low cost adsorbent for the removal of cationic dye from aqueous solution. Journal of Saudi Chemical Society, 20: S67–S76.

Faria P, Orfao J, Pereira M. (2004). Adsorption of anionic and cationic dyes on activated carbons with different surface chemistries. Water Research, 38: 2043-2052.

Fatta-Kassinos D, Kalavrouziotis I, Koukoulakis P, Vasquez M. (2011). The risks associated with wastewater reuse and xenobiotics in the agroecological environment. Science of the Total Environment, 409: 3555-3563.

Gunay A, Arslankaya E, Tosun I. (2007). Lead removal from aqueous solution by natural and pretreated clinoptilolite: adsorption equilibrium and kinetic. Journal of Hazardous materials, 146: 362-371.

Guo S, Liang X, Feng N, Tian Q. (2010). Isotherms, kinetics and thermodynamic studies of adsorption of Cu^{2+} from aqueous solutions by Mg^{2+}/K^{+} type orange peel adsorbents. Journal of Hazardous Materials, 174: 756-762.

Hansen B, Davies S. (1994). Review of potential technologies for the removal of dissolved components from produced water. Chemical engineering research & design, 72: 176-188.

Hobson JP. (1969). Physical adsorption isotherms extending from ultra-high vacuum to vapour pressure. Journal of Physical Chemistry. 73: 2720-2727.

Idoko B, Ayuba AM. (2020). Kinetic, equilibrium and thermodynamic studies on the adsorption of Crystal Violet dye from Aqueous Solution using Activated Cowpea (*Vigna Unguiculata)* Husk. Applied Journal of Enviroment Engineering Science, 6(2): 182-195.

Kolapo AL, Okunade MA, Adejumobi JA, Ogundiya MO. (2009). Phytochemical composition and antimicrobial activity of *Prosopis africana* against some selected oral pathogens. World J. Agric. Sci. 5:90-93.

Krysztafkiewicz A, Binkowski S, Jesionowski T. (2002). Adsorption of dyes on a silica surface. Applied surface science, 199: 31-39.

Kumar YP, King P, Prasad VSRK. (2006). Removal of copper from `aqueous solution using Ulva fasciata sp. Marine green algae. Journal of Hazardous Materials, 137: 367-73.

Lagergern S. (1898). About the theory of so-called adsorption of soluble substances. K. Sven. Vetenskapsakad. Handl. 24: 1-39.

Mitiku AC. (2015). Removal of 2,4-D, Atrazine and major metabolites of atrazine from aqueous solution by Fe-Zr-Mn nano composite. Msc dissertation. Haramaya University.

Mohan S, Karthikeyan J. (1997). Removal of lignin and tannin colour from aqueous solution by adsorption on to activated carbon. Environmental pollution,183-187.

Oyeyode JO, Ayuba AM. (2022). Adsorption of Methyl Orange Dye from Aqueous Solution by Carbonized Iron Tree (*Prosopis africana)* Seeds: Kinetic, Equilibrium and Thermodynamic Studies, Applied Journal of Environment Engineering Science, 8(2): 130-147.

Satish P, Vaijanta D, Sameer R, Naseema P. (2011). Kinetics of adsorption of crystal violet from aqueous solutions using different natural materials. International Journal of Environmental Science, 1: 6-19.

Tahira M, Muhammad TS, Abdul N, Paul W, Syed M, Absar A. (2011). Comparison of Different Methods for the Point of Zero Charge Determination of NiO. Ind. Eng. Chem. Res., 50: 10017–10023.

Vibhawari D, Pandey ND. (2012). Single and competitive sorption of heavy metal ions of (Cd^{2+}&Cu^{2+}) on a clayey soil. European Journal of Chemistry, 7(SI): S27-S34. Https://doi.org/10.1155/2010/710546.

Wael M, Ibrahim AF, Hassan Y, Azab A. (2016). Biosorption of toxic heavy metals from aqueous by Ulva lactuca activated carbon. Egyptian journal of basic and applied science http://dx.doi.org/10.1016/j.ejbas.2016.07.005.

Wahab MA, Boubakri H, Boubakri S, Jedidi N. (2012). J. of Hazardous Materials, 241-242(2012)101–109. doi:10.1016/j.jhazmat.2012.09.018.

Weber TN, Morris JC. (1963). Kinetics of adsorption on carbon from solution. Journal of Sanit. Engineering. Div. Proc. Am. Soc. Civil. Eng. 89: 31-59.

Yu JG, Zhao XH, Yang H, Chen Q, Yang LY, Yu JH, Jiang XQ. (2014). Aqueous adsorption and removal of organic contaminants by carbon nanotubes, Science of the Total Environment, 482: 241-251.